

The period ratio P_1/P_2 of torsional Alfvén waves with steady flows in spicules

H. Ebadi • S. Shahmorad • S. Vasheghani Farahani

Abstract The aim here is to model the standing torsional oscillations in solar spicules in the presence of density stratification, magnetic field expansion, and steady flows. By implementing cylindrical geometry, the eigenfrequencies, eigenfunctions, and the period ratio P_1/P_2 of these waves is obtained for finite plasma- β . The shifts created by the steady flow justifies the divergence of the observed period ratio for the first and second periods from the number 2.

Keywords Sun, Spicules; MHD waves, Torsional Alfvén waves; Period ratio, Steady flows

1 Introduction

The solar atmosphere is designed by beautiful magnetic structures e.g., loops, arcades, filaments, jets, spicules, etc. The evolution in the observational instruments and satellites has made the observation of these magnetic structures more and more possible over the years (Golub et al. 2007; Pesnell et al. 2012). But the concept that is of our interest is the oscillations guided by these magnetic structures. Due to the transverse structuring in the solar atmosphere

caused by these plasma eruptions, magnetohydrodynamic (MHD) waves are bound to propagate along them (Van Doorselaere et al. 2008). In the present study the magnetic structures under consideration are the spicules. Spicules are one of the most observed phenomena in the solar atmosphere especially in the chromosphere. Although spicules look very similar to coronal jets, but they are usually smaller, cooler, and denser. The chromospheric spicules observed at the solar limb are reported to have speeds around $20 - 25 \text{ km s}^{-1}$ propagating out towards the solar corona (Zaqarashvili and Erdélyi 2009). The diameter of spicules ranges from 400 km to 1500 km, and their lengths ranges from 5000 km to 9000 km. The typical lifetime of spicules is between 5 and 15 minutes, with densities between 3.5×10^{16} and $2 \times 10^{17} \text{ m}^{-3}$. Their temperatures are estimated between 5000 and 8000 K (Beckers 1968; Sterling 2000). In the context of the present study, it is the wave dynamics in spicules which is to be taken under consideration. Spicules experience transverse oscillations which have already been observed by both, spectroscopic and imaging devices. Ground based coronagraphs (Nikolsky and Sazanov 1967; Kukhianidze et al. 2006; Zaqarashvili et al. 2007) together with SOHO proved adequate for the detection of Doppler shift oscillations in spicules (Xia et al. 2005). With the enhancement of observational devices (Hinode/SOT) periodic displacements of the spicule axis became more and more pronounced, where some where interpreted as kink (Kim et al. 2008; He et al. 2009; Ebadi and Ghiassi 2014; Ebadi et al. 2012; Ebadi 2013) and some as Alfvénic waves (De Pontieu et al. 2007; Ebadi and Khoshrang 2014). However, the statistical study carried out by Okamoto and De Pontieu (2011) using Hinode/SOT showed that 59% percent of the waves guided by spicules propagate upward, 21% of the waves propagate downward, and 20% of the waves are standing oscillations. In the present study the

H. Ebadi

Astrophysics Department, Physics Faculty, University of Tabriz, Tabriz, Iran
e-mail: hosseinebadi@tabrizu.ac.ir

S. Shahmorad

Applied Mathematics Department, Mathematics Faculty, University of Tabriz, Tabriz, Iran
e-mail: shahmorad@tabrizu.ac.ir

S. Vasheghani Farahani

Department of Physics, Tafresh University, P.O. Box 39518-79611, Tafresh, Iran
e-mail: S.Vasheghanifarahani@tafreshu.ac.ir

MHD wave under consideration is the torsional Alfvén wave. Out of all the MHD waves (Edwin and Roberts 1983), only the torsional Alfvén wave is completely incompressible (Van Doorselaere et al. 2008). However Vasheghani et al. (2010) showed that in the presence of an equilibrium magnetic twist, the torsional wave becomes compressible. Observation wise, there is still vague indirect evidence of the detection of torsional Alfvén waves in the solar chromosphere and corona. This is due to lack of spatial resolution in solar observations. However, Zaqarashvili (2003); Zaqarashvili et al. (2007) studied the non-thermal broadening of the green line in a coronal loop and came to the conclusion that they are standing torsional waves. In the photosphere-chromosphere region, Jess et al. (2009) reported the periodic variations of the spectral line widths as detection of torsional waves.

One of the features of coronal seismology is the period ratio, P_1/P_2 , of the waves, where P_1 represents its fundamental period and P_2 represents its first harmonic. In this line Ebadi and Khoshrang (2014) analyzed the time series of oxygen line profiles obtained from SUMER/SOHO on the solar south limb spicules. They calculated the Doppler shifts and consequently Doppler velocities in the coronal hole region. Their wavelet analysis determined periods of the fundamental mode and first harmonic. The calculated period ratios showed departures from the canonical value of 2. The reason for this deviation could be due to two issues. One is density stratification (Andries et al. 2009), the other is magnetic twist (Karami and Bahari 2009, 2012). In other words, Van Doorselaere et al. (2007) analyzed active region observations based on TRACE instrument and detected two periods with high confidence and calculated P_1/P_2 as 1.8. Nonetheless, Ebadi and Shahmorad (2014) studied the competitive effects of density stratification and magnetic field expansion on torsional Alfvén waves in solar spicules. They showed that under some circumstances this ratio can approach its observational value even though it departs from its canonical value of 2.

In the present study, in addition to the density stratification and magnetic field expansion of the cylindrical structure which resembles a solar spicule, a steady flow parallel to the vertical magnetic field is also taken in to account. Prior to this work the effects of steady flows were studied in cylindrical structures by Goossens et al. (1992); Terra-Homem and Erdélyi (2003); Vasheghani et al. (2009) where it was shown how the steady flow makes the frequencies undergo a Doppler shift as well as shifting the cut-off frequencies. The consequence of this could be reflected in the period ratios of the oscillations in the wave guiding structure Ruderman (2010). Ebadi et al. (2012) analyzed

the observational data obtained from Hinode/SOT and performed time slice diagrams shedding more light on the spicule oscillations. In the present study the MHD waves in the presence of steady flow inside solar spicule is studied. The model is discussed in the next section.

2 Model and equilibrium conditions

Consider an expanding untwisted magnetic flux tube with varying density along its axis. If a steady flow along the axis of this tube is present, a solar spicule is resembled. It is now clear that the geometry implemented will be cylindrical with coordinates (r, φ, z) . Note that the cylinder axis is aligned with the z -axis and the equilibrium magnetic field components are B_r and B_z with no azimuthal field, ($B_\varphi = 0$). The equilibrium magnetic field, B , could be written in terms of the vector potential (A) as

$$\mathbf{A} = \frac{\psi(r, z)}{r} \hat{e}_\varphi, \quad (1)$$

where we have

$$B_r = -\frac{1}{r} \frac{\partial \psi}{\partial z}, \quad B_z = \frac{1}{r} \frac{\partial \psi}{\partial r}. \quad (2)$$

Note that ψ is taken constant along the field lines. Since the aim here is to study standing torsional Alfvén waves, we consider one node on the foot point of the spicule at $z = 0$ and the other node on the extent of the spicule at $z = L$. Note that L is the spicule length. The dynamics of such oscillations are well described by the model proposed by Ruderman (2011). If the steady flow inside the spicule is parallel to the spicule axis and represented by v_0 , we have

$$\left(\frac{\partial}{\partial t} + v_0 \frac{\partial}{\partial z} \right)^2 \xi = \frac{1}{\mu_0 \rho} (\nabla \times \mathbf{b}) \times \mathbf{B}, \quad (3)$$

and

$$\mathbf{b} = \nabla \times (\xi \times \mathbf{B}), \quad (4)$$

where the plasma displacement is $\xi = (0, \xi_\varphi, 0)$, and the magnetic field perturbation is $\mathbf{b} = (0, b_\varphi, 0)$. By considering the perturbations proportional to $\exp(-i\omega t)$, Eqs. (3) and (4) would become

$$\begin{aligned} \mu_0 \rho \left(\omega^2 + 2i\omega v_0 \frac{\partial}{\partial z} - v_0^2 \frac{\partial^2}{\partial z^2} \right) \xi_\varphi \\ + \frac{B_r}{r} \frac{\partial(r b_\varphi)}{\partial r} + B_z \frac{\partial b_\varphi}{\partial z} = 0, \end{aligned} \quad (5)$$

and

$$b_\varphi = \frac{\partial(B_r \xi_\varphi)}{\partial r} + \frac{\partial(B_z \xi_\varphi)}{\partial z}. \quad (6)$$

In the long-wavelength limit where, R , the radius of expanding spicule is much smaller than the spicule length ($R/L \ll 1$), Eqs. (5) and (6) could be combined to give

$$\mu_0 \rho \left(\omega^2 + 2i\omega v_0 \frac{\partial}{\partial z} - v_0^2 \frac{\partial^2}{\partial z^2} \right) \xi_\varphi + \frac{B_z}{R} \frac{\partial}{\partial z} \left[R^2 B_z \frac{\partial}{\partial z} \left(\frac{\xi_\varphi}{R} \right) \right] = 0. \quad (7)$$

In obtaining Equation (7) the independent variable ψ has been used instead of $r = r(\psi, z)$ by implementing the following rules

$$\begin{aligned} \frac{\partial f}{\partial r} &= r B_z \frac{\partial f}{\partial \psi} \\ \frac{\partial f}{\partial z} &= \frac{\partial f}{\partial z} - r B_r \frac{\partial f}{\partial \psi}. \end{aligned} \quad (8)$$

Now by differentiating the identities $\psi = \psi(r(\psi, z), z)$ and $r = r(\psi(r, z), z)$ with respect to z , and making use of Equation (2), one obtains

$$\begin{aligned} \frac{\partial r}{\partial z} &= \frac{B_r}{B_z} \\ \frac{\partial r}{\partial \psi} &= \frac{1}{r B_z}, \end{aligned} \quad (9)$$

see Ruderman et al. (2008); Verth et al. (2010); Karami and Ballester (2011) for details. Equation (7) is a generalization of the analysis presented by Morton et al. (2011).

In the context of coronal seismology, it would be more realistic to use the background magnetic field, plasma density, and spicule radius inferred from the actual magnetoseismology of observation (Verth et al. 2011)

$$\begin{aligned} B_z(z) &= B_0 \exp(-z/H_B) \\ \rho(z) &= \rho_0 \exp(-z/H_\rho) \\ R(z) &= R_0 \exp(z/2H_B). \end{aligned} \quad (10)$$

The third expressio of Equation 10 is due to the conservation of the magnetic flux, where H_B and H_ρ are the magnetic and density scale heights, respectively. substituting Eqs. (10) in Equation (7) gives

$$\begin{aligned} & (1 - M_A^2 e^{-\alpha z}) \frac{\partial^2 \xi_\varphi}{\partial z^2} + \\ & \left(4\pi i M_A e^{-\alpha z} - \frac{1}{H_B} \right) \frac{\partial \xi_\varphi}{\partial z} + \\ & \left(\frac{1}{4H_B^2} + 4\pi^2 \omega^2 e^{-\alpha z} \right) \xi_\varphi = 0, \end{aligned} \quad (11)$$

where $\alpha \equiv \left(\frac{H_B - 2H_\rho}{H_\rho H_B} \right)$ and $M_A \equiv \frac{v_0}{v_A}$. In Equation (11) the lengths are normalized by the spicule length (L), and the frequencies by the Alfvén frequency ($\omega_A \equiv \frac{v_A}{L} = 0.06$ rad/s). The other parameters are as; $v_A = \frac{B_0}{\sqrt{\mu_0 \rho_0}} = 75$ km/s; $B_0 = 12$ G, $\rho_0 = 1.9 \times 10^{-10}$ kg m⁻³, $\mu_0 = 4\pi \times 10^{-7}$ T m A⁻¹, and $L = 8000$ km). The magnetic and density scale heights have been determined by Verth et al. (2011) as $H_B = 0.1135$ and $H_\rho = 0.094$, respectively.

3 Numerical results and Discussions

The numerical study carried out here is based on the differential transform method (DTM (Erturk et al. 2012; Nazari and Shahmorad 2010)). This method is applied to Equation (11) which gives the eigenfrequencies and eigenfunctions of standing torsional Alfvén waves in stratified and expanding solar spicules, see Ebadi and Shahmorad (2014) for detailed description of this method.

We apply the rigid boundary conditions and assume that $\xi_\varphi(0) = \xi_\varphi(L) = 0$. In the top panel of Figure 1 the fundamental frequency ($n = 1$) of the torsional Alfvén wave is plotted with respect to the parameter α for various Mach numbers. This has been repeated for the second harmonic and shown in the middle panel of Figure 1. It could be readily noticed by comparing the corresponding curves of the top and middle panels of Figure 1 that their ratios are away from number 2. Now to give an exact flavor, the period ratios of the first and second harmonics, P_1/P_2 , are plotted in the bottom panel of Figure 1.

As it is expected, the frequencies are shifted not only because of the flow, but also because of stratification and tube expansion (Ebadi et al. 2012). In other words, their variations respect to α are very moderate. Both the effects of stratification as well as the tube expansion are quite strong. However they act in the opposite directions. While the stratification results in the reduction of the ratio P_1/P_2 , the tube expansion leads to the increase of this ratio. As a result, the two effects almost cancel each other. We can observe that they exactly cancel each other when $H_B = 2H_\rho$.

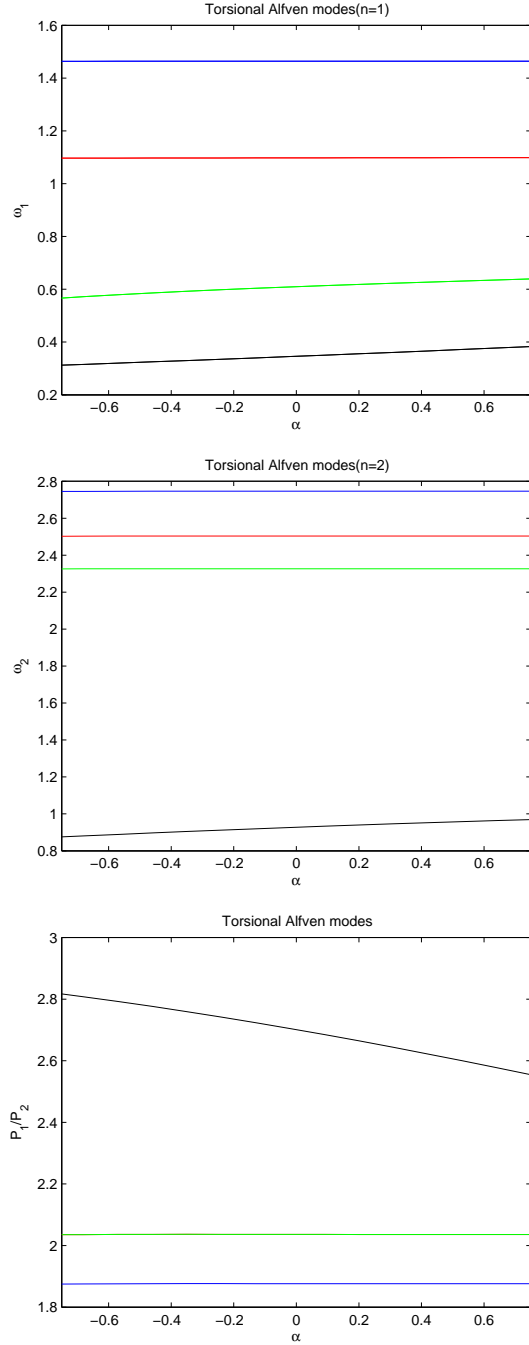


Fig. 1 Top panel, the fundamental torsional Alfvén wave frequency for Mach numbers equal to $M_A = 0, 0.2, 0.3, 0.4$ plotted against the parameter α . Middle panel, the second harmonic frequency plotted against the parameter α . The bottom panel, the period ratio P_1/P_2 of the fundamental P_1 and second harmonic period P_2 of the torsional wave against the parameter α . Note that the colors black, blue, red, and green correspond to $M_A = 0, 0.2, 0.3, 0.4$, respectively.

It could be noticed that slower steady flows create higher frequencies and consequently lower periods with respect to those of static medium. An interesting result which is obtained by looking at the bottom panel of Figure 1 is that the period ratio, P_1/P_2 , is very close to the observed values. This is due to the consideration of the steady flows in the analysis. As a matter of fact, in the case of Mach numbers equal to 0.2 and 0.3 the results are in very good agreement with observational results. It should be emphasized that steady flows have already been reported in observations carried out on spicules.

Eigenfunctions of the fundamental and first harmonic torsional Alfvén modes with respect to the normalized height along the spicule are presented in Figure 2. We plotted eigenfunctions for $H_B = 0.1135$, $H_\rho = 0.094$, and $M_A = 0.25$ which is determined by observations.

4 Conclusion

In the context of coronal seismology the aim is to understand the aspects of a phenomenon taking place in the corona by means of waves. The phenomenon under consideration in this study is the solar spicules and the wave for studying it is the torsional Alfvén wave. The models that we implemented to study the spicule is an expanding untwisted magnetic flux tube with varying density along its axis with a steady flow. The coordinates implemented for modeling the spicule was cylindrical (r, φ, z) .

By implementing cylindrical geometry, the eigenfrequencies, eigenfunctions, and the period ratio P_1/P_2 of standing torsional waves was obtained based on the observational data provided by Verth et al. (2011) for finite plasma- β . The shifts created by the steady flow justifies the divergence of the observed period ratio for the first and second periods from the number 2. By plugging in the model, actual observed data of the background magnetic field, plasma density, and spicule radius; the eigenfrequencies, eigenfunctions, and the period ratio P_1/P_2 of standing torsional waves were estimated. An interesting result obtained is that the period ratio, P_1/P_2 , is very close to the observed values. This is because of taking in to account the effects of steady flows in the analysis. As a matter of fact, in the case of Mach numbers equal to 0.2 and 0.3 the results get very close to observations. The interplay of stratification and equilibrium steady flow proved that the steady flow is something not to neglect. The good agreement of the numerical results obtained in this study with observations proof the efficiency of the steady flow effects compared to stratification.

Acknowledgements This work is published as a part of the research project supported by the University of Tabriz research affairs office. Authors thank anonymous referee for his/her useful comments in improving the article.

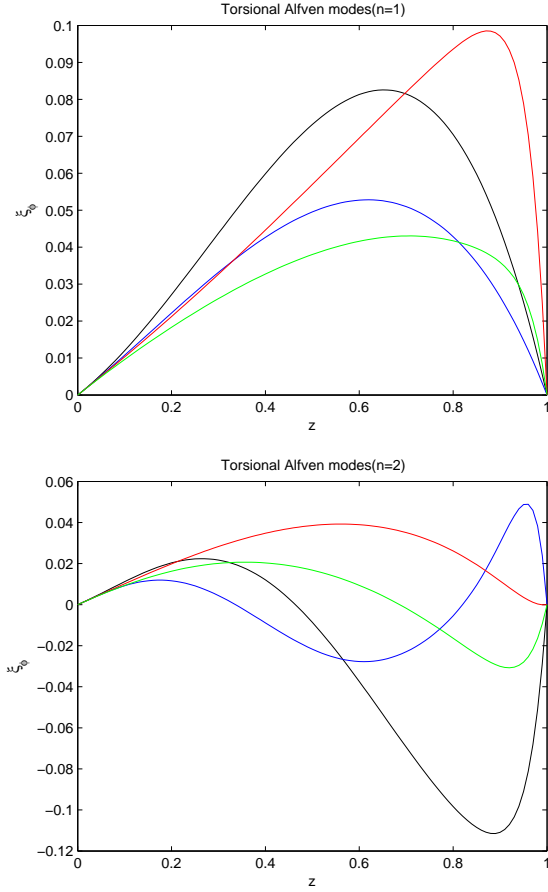


Fig. 2 Eigenfunctions of the fundamental and first harmonic torsional Alfvén waves are plotted with respect to the normalized height along the spicule. The top panel corresponds to the fundamental oscillation where the bottom panel corresponds to the second harmonic. Note that the values of the parameter α and M_A have been taken equal to 1.84 and 0.25, respectively. The order of colors are the same as of Figure 1.

References

- Andries, J., van Doorselaere, T., Roberts, B., Verth, G., Verwichte, E., Erdélyi, R.: 2009 *Space Sci. Rev.* **149**, 3.
- Beckers, J.M.: 1968, *Sol. Phys.* **3**, 367.
- De Pontieu, B., McIntosh, S.W., Carlsson, M., et al.: 2007, *Science*, **318**, 1574.
- Ebadi, H.: 2013, *Astrophys. Space Sci.* **348**, 11.
- Ebadi, H., Ghiassi, M.: 2014, *Astrophys. Space Sci.*, **353**, 31.
- Ebadi, H., Khoshrang, M.: 2014, *Astrophys. Space Sci.*, **352**, 353.
- Ebadi, H., Shahmorad, S.: 2014, *Astrophys. Space Sci.*, **353**, 25.
- Ebadi, H., Zaqarashvili, T.V., Zhelyazkov, I.: 2012a, *Astrophys. Space Sci.*, **337**, 33.
- Ebadi, H., Zaqarashvili, T.V., Zhelyazkov, I.: 2012b, *AIP Conference Proceedings*, **1356**, 117.
- Edwin, P.M., Roberts, B. 1983, *Sol. Phys.*, **88**, 179.
- Erturk, V.S., Odibat, Z.M., Momani, S.: 2012, *The Adv. Appl. Math. Mech.*, **4**, 422.
- Golub, L., Deluca, E., Austin, G., et al. 2007, *Sol. Phys.*, **243**, 63.
- Goossens, M., Hollweg, J. V., Sakurai, T. 1992, *Sol. Phys.*, **138**, 233.
- He, J., Marcsh, E., Tu, G., Tian, H.: 2009, *Astrophys. J. Lett.*, **705**, 217.
- Jess, D.B., Mathioudakis, M., Erdélyi, R., Crockett, P.J., Keenan, F.P., Christian, D.J.: 2009, *Science*, **323**, 1582.
- Karami, K., Bahari, K.: 2012, *Astrophys. J.*, **757**, A86.
- Karami, K., Bahari, K.: 2011, *Astrophys. Space Sci.*, **333**, 463.
- Karami, K., Bahari, K.: 2009, *Mon. Not. R. Astron. Soc.*, **394**, 521.
- Kim, Y.H., Bong, S.C., Park, Y.D., Cho, K.S., Moon, Y.J., Suematsu, Y.: 2008, *J. Korean Astron. Soc.*, **41**, 173.
- Kukhianidze, V., Zaqarashvili, T.V., Khutsishvili, E.: 2006, *Astron. Astrophys.*, **449**, 35.
- Morton, R.J., Ruderman, M.S., Erdélyi, R.: 2011, *Astron. Astrophys.*, **534**, A27.
- Nazari, D., Shahmorad, S.: 2010, *J. Comp. Appl. Math.*, **234**, 883.
- Nikolsky, G.M., Sazanov, A.A.: 1967, *Soviet Astron.*, **10**, 744.
- Okamoto, T.J., De Pontieu, B.: 2011, *Astrophys. J.*, **736**, L24.
- Pesnell, W. Dean, Thompson, B.J., Chamberlin, P.C. 2012, *Sol. Phys.*, **275**, 3.
- Ruderman, M.S.: 2010, *Sol. Phys.*, **267**, 377.
- Ruderman, M.S.: 2011, *Astron. Astrophys.*, **534**, A78.
- Ruderman, M.S., Verth, G., Erdélyi, R.: 2008, *Astrophys. J.*, **686**, 694.
- Sterling, A.C.: 2000, *Sol. Phys.*, **196**, 79.
- Terra-Homem, M. & Erdélyi, R.: 2003, *Sol. Phys.*, **217**, 199.
- Vasheghani Farahani, S., Van Doorselaere, T., Verwichte, E., Nakariakov, V.M. 2009, *Astron. Astrophys.*, **498**, L29.
- Vasheghani Farahani, S., Nakariakov, V.M., Van Doorselaere, T. 2010, *Astron. Astrophys.*, **517**, A29.
- Van Doorselaere, T., Nakariakov, V. M., Verwichte, E. 2008, *Astrophys. J.*, **676**, L73.
- Van Doorselaere, T., Brady, C.S., Verwichte, E., and Nakariakov, V.M. 2008, *Astron. Astrophys.*, **491**, L9-L12.
- Van Doorselaere, T., Nakariakov, V. M., Verwichte, E. 2007, *Astron. Astrophys.*, **473**, 959.
- Verth, G., Erdélyi, R., Goossens, M.: 2010, *Astrophys. J.*, **714**, 1637.
- Verth, G., Goossens, M., He, J.-S.: 2011, *Astrophys. J. Lett.*, **733**, 15.
- Xia, L.D., Popescu, M.D., Doyle, J.G., Giannikakis, J.: 2005, *Astron. Astrophys.*, **438**, 1152.
- Zaqarashvili, T.V.: 2003, *Astron. Astrophys.*, **399**, 15.
- Zaqarashvili, T.V., Erdélyi, R.: 2009, *Space Sci. Rev.* **149**, 335.
- Zaqarashvili, T.V., Khutsishvili, E., Kukhianidze, V., Ramishvili, G.: 2007, *Astron. Astrophys.*, **474**, 627.